



Large-volume and room-temperature gamma spectrometer for environmental radiation monitoring

Romain Coulon, Jonathan Nicolas Dumazert, Tola Tith, Emmanuel Rohée,
Karim Boudergui

► To cite this version:

Romain Coulon, Jonathan Nicolas Dumazert, Tola Tith, Emmanuel Rohée, Karim Boudergui. Large-volume and room-temperature gamma spectrometer for environmental radiation monitoring. Nuclear Engineering and Technology, 2017, 49 (7), pp.1489 - 1494. 10.1016/j.net.2017.06.010 . hal-01878815

HAL Id: hal-01878815

<https://hal.science/hal-01878815>

Submitted on 28 Jun 2023

HAL is a multi-disciplinary open access archive for the deposit and dissemination of scientific research documents, whether they are published or not. The documents may come from teaching and research institutions in France or abroad, or from public or private research centers.

L'archive ouverte pluridisciplinaire **HAL**, est destinée au dépôt et à la diffusion de documents scientifiques de niveau recherche, publiés ou non, émanant des établissements d'enseignement et de recherche français ou étrangers, des laboratoires publics ou privés.



Original Article

Large-volume and room-temperature gamma spectrometer for environmental radiation monitoring

Romain Coulon*, Jonathan Dumazert, Tola Tith, Emmanuel Rohée, Karim Boudergui

CEA, LIST, F-91191 Gif-sur-Yvette Cedex, France

ARTICLE INFO*Article history:*

Received 29 April 2016

Received in revised form

15 May 2017

Accepted 4 June 2017

Available online 3 July 2017

Keywords:

Xenon

Spectrometry

Environmental

Detector

Radiation

Ionization chamber

ABSTRACT

The use of a room-temperature gamma spectrometer is an issue in environmental radiation monitoring. To monitor radionuclides released around a nuclear power plant, suitable instruments giving fast and reliable information are required. High-pressure xenon (HPXe) chambers have range of resolution and efficiency equivalent to those of other medium resolution detectors such as those using NaI(Tl), CdZnTe, and LaBr₃:Ce. An HPXe chamber could be a cost-effective alternative, assuming temperature stability and reliability. The CEA LIST actively studied and developed HPXe-based technology applied for environmental monitoring. Xenon purification and conditioning was performed. The design of a 4-L HPXe detector was performed to minimize the detector capacitance and the required power supply. Simulations were done with the MCNPX2.7 particle transport code to estimate the intrinsic efficiency of the HPXe detector. A behavioral study dealing with ballistic deficits and electronic noise will be utilized to provide perspective for further analysis.

© 2017 Korean Nuclear Society. Published by Elsevier Korea LLC. This is an open access article under the CC BY-NC-ND license (<http://creativecommons.org/licenses/by-nc-nd/4.0/>).

1. Introduction

Gamma spectroscopy can be used to provide isotopic information about radioactivity. This identification then allows the diagnosis of a situation using information given by the nature of the radioactive materials. To discriminate between different isotopes with high efficiency and reliability, the energy resolution has to be as low as possible. The lowest possible resolution can be achieved by cryogenic detectors (high-purity germanium detectors), which are expensive and not suitable for use outdoors. A room temperature gamma spectrometer with quite good resolution has been developed during the last decades. CdZnTe semiconductors and LaBr₃:Ce scintillators provide an energy resolution of around 2–4% at 662 keV [1,2]. However, their cost increases dramatically with the volume and these devices need to be stabilized against external temperature variation.

Therefore, the high-pressure xenon (HPXe) technology is investigated for the CEA LIST for these problematic environmental conditions. The state of development is presented in this paper.

2. State of the art

HPXe chambers have been under development by many laboratories since the 1980s. The element xenon is a noble gas with a high charge number; xenon facilitates good gamma stopping power when used under pressure. At 50 bar, the density reaches 0.5 g/cm³ and gamma ray stopping power has a value between those of germanium and sodium iodine. Another interesting particularity is the process for charges carrier creation and, more specially, the Fano factor of this process (0.13) [3]. The intrinsic energy resolution is three times lower than those of room-temperature inorganic scintillators using NaI(Tl) or LaBr₃:Ce [4]. To address the industrial need for room temperature spectrometers, xenon is thus an important research path.

To build a spectroscopy-grade HPXe detector, some requirements have to be taken into account. The properties of the xenon gas for spectroscopy have been studied in detail by Dmirtrenko et al. [5] and Bolotnikov and Ramsey [6].

3. General properties

Thanks to electronic band evolution of Xe₂^{*} dimers (decrease of excited states compared with ionizing states) according to gas density, the W-value decreases as the gas pressure increases [6–8]. The increase of the charge carrier number and the gamma ray

* Corresponding author.

E-mail address: romain.coulon@cea.fr (R. Coulon).

stopping power are the main motives to apply very high pressure to the xenon chamber. However, a discrepancy of the energy resolution is observed when the density gets above 0.55 g/cm^3 [5]. The intrinsic energy resolution is approximately equal to 0.6% until a density value of 0.55 g/cm^3 is reached; the intrinsic energy resolution then increases to 5% at a density value of 1.6 g/cm^3 . Above 0.55 g/cm^3 the Fano factor increases (due to δ -ray recombination) and small liquid droplets appear and lead to electronegative clusters, which absorb electrons with kinetic energy below the ionizing energy level [6,9].

In practice, the pressure has to be between 0.5 g/cm^3 and 0.6 g/cm^3 . A device is exempt from French regulation rules if the pressure volume product does not exceed 200 bar L [10]. A 4-L chamber could then be built without the requirement of periodic control. The gamma ray stopping power obtained in a 4-L chamber makes possible the use of an HPXe chamber for environmental radiation monitoring.

Stability against temperature change is an issue for many industrial applications. Other room-temperature probes such as scintillators or CdZnTe suffer from temperature dependency, which affects the gain and the energy resolution. At relatively low pressure ($<0.6 \text{ g/cm}^3$), xenon shows perfect temperature stability in terms of density and charge carrier collection [6,9,11]. This particularity remains the main advantage of HPXe chambers in comparison with other room temperature spectrometers, which require temperature stabilization.

The use of an HPXe chamber could offer a gain in temperature stability and a cost reduction compared with other conventional systems. The first requirement to operate as a spectrometer is the achievement of a high purity level of xenon gas.

4. Xenon purification and conditioning

To avoid charge recombination, electronegative impurities (mainly oxygen) have to be filtered out. A purity level below parts per billion has to be achieved. Xenon with a purity level below 10 ppm is the best purity grade of commercially available purity-grade xenon (research grade). Thus, a dedicated purification process has to be built to achieve this extra level of purity. The system under development at CEA LIST is shown in Fig. 1.

The process circuit is preliminarily set to an ultravacuum level of 10^{-11} bar and temperature of 175°C is applied to cause the overall internal skin to desorb. The research-grade xenon is injected and then transferred through a purifier to the container. Xenon

displacement is ensured by the vaporization/condensation cycles, which are controlled by cryo-cooling (LN_2). A gatekeeper filter (Entegris, Billerica, MA, USA) is installed in the CEA LIST device. This filter is based on a metal alloy using chemisorption to remove impurities. It operates at room temperature but requires precise flow rate control. The gas reaches a sub-parts per billion level after many purification cycles. Spark purification, because it is fast and effective, is currently the best purification technique [12]. Spark discharge produces ultraclean titanium dust that traps electronegative impurities and organics.

The purity monitor measures the electron lifetime in the gas. An electron cloud between the two plate electrodes, which are weakly polarized (recombination mode 10 V/cm), is created by external stimulation using a gamma source. The pulse length at the output of the slow charge preamplifier has to reach a value above 5 ms to validate the sub-parts per billion level of the xenon gas [13].

When the xenon gas has reached the sub-parts per billion purity level, the detector volume can be filled. The density has to be strictly controlled. The pressure and the temperature of the gas can be measured at the end of the process. Then, the density is evaluated using an isothermal abacus [13]. Instrumentation has to guarantee a relative accuracy below 1%. Another approach to density measurement consists of dielectric constant measurement, which is a function only of the density [12]. The purity control chamber (fast charge preamplifier) can be used for capacitance measurement after a calibrated pulse generation.

Saturation level of charge collection and optimal charge drift velocity are achieved using an adequate polarization voltage. This voltage is a function of the xenon density and temperature [9]. Complete saturation is achieved using a voltage equal to 7 kV/cm , regardless of the xenon density. In practice, and especially for large volume detectors, a voltage value of 2 kV/cm has been recommended by C. Levin [14] as the best compromise.

The drift velocity has to be maximized from a dynamic range point of view but also in terms of electronic noise filtering (signal-to-noise ratio). The addition of a polyatomic quencher has been studied by V. Dmitrenko [15]. Hydrogen (H_2) is the candidate that is most compatible with purification techniques. A hydrogen concentration addition of 0.2–0.3% increases the drift velocity by a factor of 6, without degradation of the spectroscopic performance [16,17]. However, the quencher is efficient at a bias voltage above 7 kV/cm and the HPXe chamber remains as a slow detector in comparison to scintillators or cadmium zinc telluride (electron mobility equal to $1 \text{ mm}/\mu\text{s}$ in pure xenon).

5. Chamber design for the spectrometer

Parallel-plate chambers with Frisch grids comprised the first design of HPXe technology. A 17-L chamber called Kseniya was built by the National Nuclear Research University (MEPhy) in the early 1980s for space radiation measurement [18,19]. It was installed on the MIR station and operated for 11 years, maintaining a stable energy resolution (3.5% at 662 keV) in severe conditions in terms of temperature gradient and cosmic irradiation flux [20]. In the 1990s, parallel plate chambers with Frisch grids were developed in the United States for earth applications [14]. The small volume of 0.16 L permitted the achievement of an energy resolution of 2.5% at 662 keV, but some limits were noted for industrial applications [21,22]. The useful volume of gas was only 30% due to the electric field inhomogeneity effect. As such, a large dead area produced an important Compton continuum in the gamma spectrum. Moreover, the Frisch grid structure induced additional acoustic noise. The cylindrical chambers allowed an optimization of the useful volume of gas (close to 100%), but vibration sensitivity remained a problem. To limit the acoustic noise, the Frisch grid has to be made with

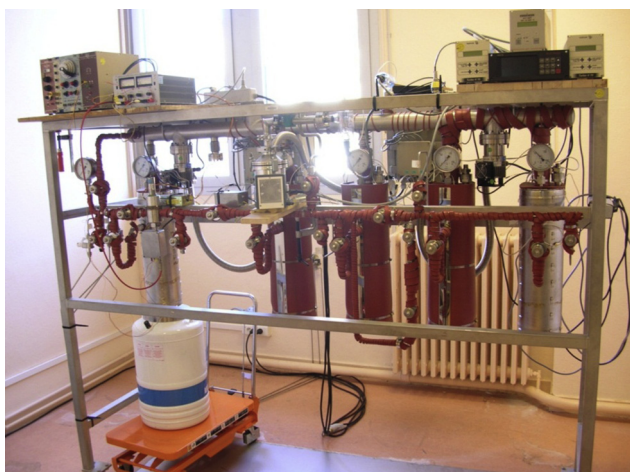


Fig. 1. Xenon purification apparatus of CEA LIST.

stainless steel or nickel-electroformed meshes and must be self-supporting.

Cylindrical chambers without Frisch grids have been developed by MEPhI (0.9 L and 5 L) [23]. Exceptional reliability has been observed in severe conditions of use. The chamber is insensitive to industrial vibration, as was found when device was tested in an MI-8 helicopter [24]. The chamber can operate without discrepancy up to 180°C. This spectrometer has been tested for geophysical prospection at an operating temperature of 150°C and by a KCl fertilizer manufacturer at an operating temperature of 120°C [25].

The ballistic deficit (pulse shape dependency with interaction locations) plays a role in the discrepancy of the energy resolution. The ion drift velocity is one thousand times higher than the electron velocity. This phenomenon induces a position dependency of the pulse amplitude. The ballistic deficit can be neglected for small volume detectors but becomes predominant in large volume detectors. A small volume chamber exhibits a resolution equivalent to that of NaI(Tl) chambers (8% at 662 keV). The ballistic effect in a large volume chamber is the first technological challenge for the application under consideration.

6. Ballistic deficit

Traditionally, this effect is corrected for by setting the Frisch grid closer to the anode. As a result, the anode is shielded against the ion contribution [16,24]. Cylindrical chambers with Frisch grids are efficient, allowing the achievement of the best possible energy resolution (close to 2% at 662 keV). However, the use of a Frisch grid is not suitable for industrial applications due to vibration sensitivity. Thus, alternatives to Frisch grids are under investigation. CdZnTe diodes are subject to the same problems regarding electron/hole motion. Options to deal with the ballistic deficit are inspired by options that have been used to deal with the CdZnTe ballistic deficit.

6.1. Biparametric correction

Biparametric correction has been developed for CdTe detectors. The CEA LIST has tested the direct use of the CdTe algorithm [26,27]. The correction has permitted a slight resolution improvement of 14%.

Xenon gas is also a scintillator, emitting vacuum ultraviolet fluorescence photons at a wavelength of 173 nm and with a light efficiency equal to 40,000 photons/MeV at 0.19 g/cm³ [28]. In practice, light collection is difficult to extract but this light signal could be used as a trigger. A primary scintillation light is produced during charge carrier creation. If the electrical field around the anode is above 2.9×10^{-17} V/cm², another type of light is produced by the electroluminescence effect. The primary scintillation light (fluorescence) is produced along the interaction path. The stimulated scintillation light (electroluminescence) is emitted at the end of the charge collection. The scintillation pulse signal has an excellent time resolution compared with that of the charge pulse. The light pulse is composed of two kinds of scintillation, which allows an accurate measurement of the charge collection time. This particularity was extended to astrophysics experiments in HPXe-time projection chamber (HPXe-TPC) for research into dark matter or weakly interacting massive particles [29–31]. This chamber could also be used as a gamma Compton imagers [32,33]. For gamma spectroscopy concerns, which are under investigation, the use of a scintillation pulse provides an improvement in the biparametric correction of the charge pulse [34]. Using this new information and a compensation algorithm dedicated to HPXe, J.L. Lacy et al. [35] (Proportional Technology Inc.) have made an improvement of ballistic

effect compensation. The company's 0.3-L chamber maintains a low capacitance of 7 pF and its correction algorithm permits the achievement of an energy resolution equal to 2.3% at 511 keV (very close to that of the Frisch grid technology).

6.2. Other approaches

The coplanar anode configuration has been investigated to compensate for the ballistic deficit of currently used CdZnTe diodes [36].

A double anode design has been proposed by Bolotnikov et al. [16] in which only one anode is polarized. It is assumed that only one anode collects the electrons, whereas both anodes are exposed to the current induced by the ion collection. The subtraction of the anode signal gives, in theory, a signal without ionic component. In practice, the process of ballistic compensation is not efficient due to a supposed self-shielding effect between the anodes. Other coplanar anode structures have been developed without significant success [37].

A virtual Frisch grid has also been developed by Bolotnikov et al. [38] and Austin [39] (Constellation Technology Corp.). The chamber is composed of two plate electrodes embedded in a cylindrical ceramic conductor. This device is based on the principle that electron collection is performed by the plate anode and the ions are trapped by the ceramic. This design produced convenient results (energy resolution in the range of 2–2.5% at 662 keV) but it is not scalable to larger volumes. To increase the chamber volume, segmentation of the virtual Frisch grid is under study [39].

Lacy technology is the best method of correcting the deficit ballistic, but there are currently no efficient methods to manage the ballistic deficit in a large-volume HPXe chamber.

The second technological barrier for spectroscopy in a large volume chamber is minimizing and filtering the electronic noise.

7. Electronic noise

Electronic noise contributions are important parts of the energy resolution. Although intrinsic energy resolution is about 0.5%, total energy resolution is in the best cases close to 2%. Electronic noise (and acoustic noise) is critical in HPXe compared with other detectors due to this detector's high W-value and its low charge mobility. Electronic noise is mainly induced by thermal agitation in the capacitance formed by the chamber. Its variance \bar{Q}^2 is proportional to the temperature T and the detector capacitance C , as described below, where k_B is the Boltzmann constant.

$$\bar{Q}^2 = k_B T C \quad (1)$$

The distance between the anode and cathode has to be maximized to minimize the capacitance. In cylindrical geometry, the capacitance can be calculated as presented in Eq. (2), where l is the chamber length, R_1 is the anode radius, R_2 is the cathode radius, and ω_0 and ω_r are, respectively, the strength of the vacuum and the relative dielectric permittivity. The chamber should be designed with a length that is larger than its diameter, as is obvious from Eq. (2).

$$C = 2\pi\omega_0\omega_r \frac{l}{\ln\left(\frac{R_2}{R_1}\right)} \quad (2)$$

The junction field effect transistors of the front-end electronics has to be carefully chosen, with a low gate current noise. Finally, the shaping time constant of the triangular/trapezoidal filter has to be adjusted to increase the signal-to-noise ratio. It should be noted

that the signal-to-noise ratio has to be optimized at an earlier stage of the chain by adaptive quencher incorporation and suitable electrode design.

Electronic noise reduction is an important requirement to be considered in HPXe chamber design. Many authors have been disappointed by detector capacitance limiting the resolution of their systems [37,40,41]. In the best cases, a capacitance in the range of 5 pF to 10 pF is achieved. Some designs are under study to achieve very low capacitance. A segmented anode was developed by Kiff et al. [37,42] and Bolotnikov [43] to reduce the capacitance to a value below 5 pF [37,42,43].

Advanced signal processing (nonlinear filter) could also be envisaged. The CEA LIST has developed a nonlinear filter for gamma spectroscopy signal processing [44]. Optimal noise filtering can be achieved and a spectroscopic response free of ballistic effect is allowed thanks to accurate knowledge of the charge collection time. This signal processing solution is a promising one for dealing with the two technological barriers of large-volume chambers: the electronic noise and the ballistic effect.

8. Simulation

Design of a 4-L HPXe is performed to minimize the detector capacitance and the required power supply. Figs. 2 and 3 show the bias voltage needed to maintain the capacitance at 2 kV/cm; the capacitance evolution is a function of the cylindrical length to the diameter ratio. An internal anode with a diameter equal to 1 mm is considered.

It is impossible in a large volume cylindrical chamber to reach a very low capacitance. The target resolution cannot be the same as that of a small detector (2%) but can reach the resolution of reference NaI(Tl) detectors (7–8%).

A compromise is found for a length-to-diameter ratio equal to unity. This ratio also provides a way to optimize the isotropic response of the detector.

Geometrical and electrical characteristics of the 4-L cylindrical chamber are as follows:

- Diameter: 17 cm
- Length: 17 cm
- Bias voltage: 17 kV
- Capacitance: 27 pF

Simulations were done by MCNPX2.7 particle transport code [45]. The intrinsic efficiency is estimated for a large-volume and medium-resolution gamma spectroscopy detector. As shown in

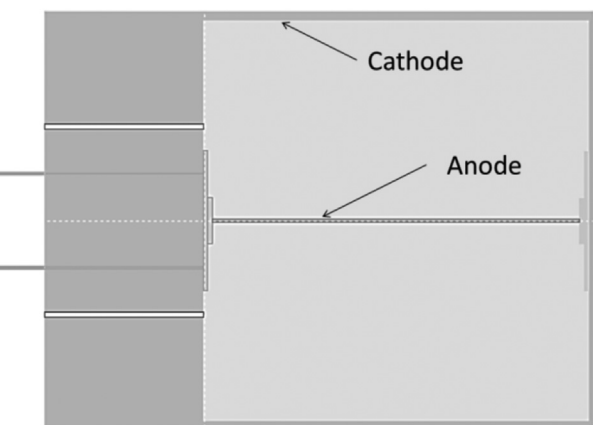


Fig. 3. Geometry of an environmental HPXe chamber.

Fig. 4, the HPXe chamber can obtain a gamma ray efficiency close to those of other, large-volume technology devices.

9. Conclusion

A 4-L HPXe chamber is under study at the CEA LIST for environmental radiation monitoring. A simulation study has been conducted and has allowed us to conclude that the chamber can exhibit an intrinsic resolution equivalent to that of the largest volume detectors made using competitive technology.

Xenon purification and conditioning were performed. The design of the 4-L HPXe detector was done to minimize the detector capacitance and the required power supply. Simulations were done using the MCNPX2.7 particle transport code to estimate the intrinsic efficiency of the HPXe detector.

Future research will address ballistic deficit issues and accurate measurement of charge drift time.

The first investigation will consist of coupling the chamber with a vacuum ultraviolet-sensitive photomultiplier and delimiting the charge drift on the primary and secondary (electroluminescent) scintillations.

A second study will investigate spherical xenon proportional counters, designed to maximize the homogeneity of the charge multiplication in the sensitive medium. Such a technology, thanks to the Townsend avalanche phenomenon [46], would reduce the ballistic deficit and the electronic noise, improving the signal-to-noise ratio and suppressing ion contribution to the signal.

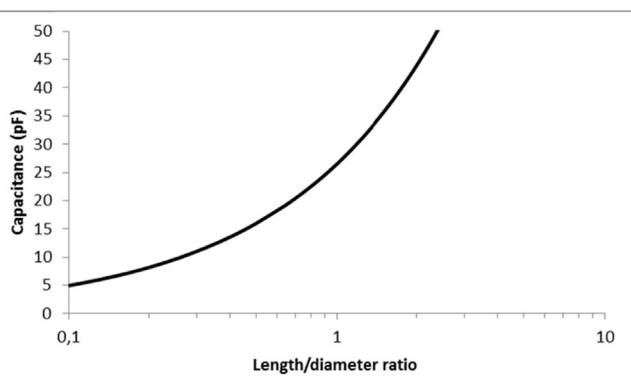
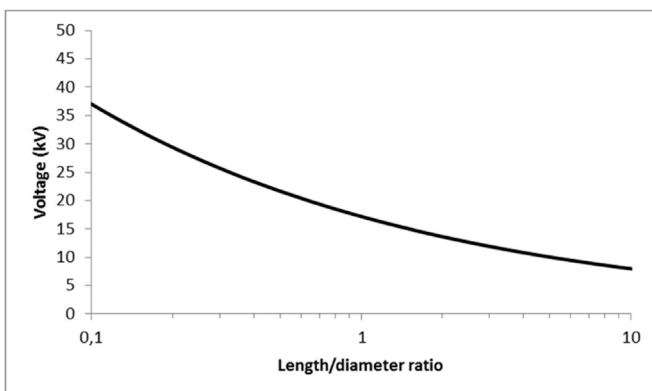


Fig. 2. Bias voltage and capacitance versus length/diameter ratio.

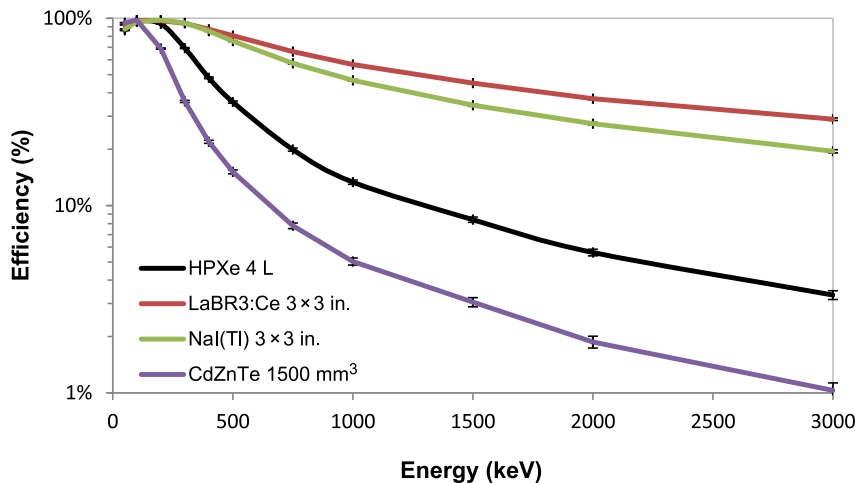


Fig. 4. Intrinsic efficiency as a function of the incident gamma ray energy.

Conflicts of interest

The authors have no conflicts of interest to declare.

References

- [1] S. Normand, A. Iltis, F. Bernard, T. Domenech, P. Delacour, Resistance to γ irradiation of LaBr₃:Ce and LaCl₃:Ce single crystals, Nucl. Instrum. Methods Phys. Res. A 572 (2007) 754–759.
- [2] J. Dumazert, R. Coulon, V. Kondrasovs, K. Boudergui, Compensation scheme for online neutron detection using a Gd-covered CdZnTe sensor, Nucl. Instrum. Methods Phys. Res. A 857 (2017) 7–15.
- [3] U. Fano, Ionization yield of radiations. II. The fluctuations of the number of ions, Phys. Rev. 72 (1947) 26–29.
- [4] D.F. Anderson, T.T. Hamilton, W.H.-M. Ku, R. Novick, A large area, gas scintillation proportional counter, Nucl. Instrum. Methods 163 (1979) 125–134.
- [5] V.V. Dmitrenko, A.S. Romaniuk, S.I. Suchkov, Z.M. Uteshev, Electron mobility in dense xenon gas, Sov. Phys. Tech. Phys. 28 (1983) 1440–1444.
- [6] A. Bolotnikov, B. Ramsey, The spectroscopic properties of high-pressure xenon, Nucl. Instrum. Methods Phys. Res. A 396 (1997) 360–370.
- [7] P. Laporte, I.T. Steinberger, Evolution of excitonic bands in fluid xenon, Phys. Rev. A 15 (1977) 2538–2544.
- [8] P. Laporte, V. Saile, R. Reininger, U. Asaf, I.T. Steinberger, Photoionization of xenon below the atomic ionization potential, Phys. Rev. A 28 (1983) 3613.
- [9] S.-S. Huang, G.R. Freeman, Electron mobilities in gaseous, critical, and liquid xenon: density, electric field, and temperature effects: quasilocalization, J. Chem. Phys. 68 (1978) 1355–1362.
- [10] République Française. Secrétariat d'état à la l'industrie. Arrêté du 15 mars 2000 relatif à l'exploitation des équipements sous pression.
- [11] C.R. Gruhn, R. Loveman, A review of the physical properties of liquid ionization chamber media, IEEE Trans. Nucl. Sci. 26 (1979) 110–119.
- [12] A. Bolotnikov, B. Ramsey, Purification techniques and purity and density measurements of high-pressure Xe, Nucl. Instrum. Methods Phys. Res. A 383 (1996) 619–623.
- [13] O. Sifner, J. Klomfar, Thermodynamic properties of xenon from the triple point to 800 K with pressures up to 350 MPa, J. Phys. Chem. Ref. Data 23 (1994) 63–152.
- [14] C. Levin, J. Germani, J. Markey, Charge collection and energy resolution studies in compressed xenon gas near its critical point, Nucl. Instrum. Methods Phys. Res. A 332 (1993) 206–214.
- [15] V.V. Dmitrenko, A.S. Romaniuk, Z.M. Uteshev, Compressed xenon as working medium for detection of low energy gamma quanta, in: Elementary Particles and Cosmic Rays, vol. 5, Atomizdat, Moscow, Russia, 1980, pp. 72–83.
- [16] A. Bolotnikov, A. Bolozdyna, R. DeVito, J. Richards, Dual-anode high-pressure xenon cylindrical ionization chamber, IEEE Trans. Nucl. Sci. 51 (2004) 1262–1269.
- [17] S. Kobayashi, N. Hasebe, T. Igarashi, M.-N. Kobayashi, T. Miyachi, M. Miyajima, H. Okada, O. Okudaira, C. Tezuka, E. Yokoyama, T. Doke, E. Shibamura, V.V. Dmitrenko, S.E. Ulin, K.F. Vlasik, Scintillation luminescence for high-pressure xenon gas, Nucl. Instrum. Methods Phys. Res. A 531 (2004) 327–332.
- [18] V.V. Dmitrenko, V.N. Lebedenko, A.S. Romaniuk, Z.M. Uteshev, Priby i Tekhnika Eksperimenta 5 (1981) 49–51 [in Russian].
- [19] V.V. Dmitrenko, V.N. Lebedenko, A.S. Romaniuk, Priby i Tekhnika Eksperimenta 5 (1982) 51–53 [in Russian].
- [20] S.E. Ulin, K.F. Vlasik, K.F. Galper, V.M. Dmitrenko, V.I. Liagushin, Z.M. Uteshev, Yu T. Yurkin, Influence of proton and neutron fluxes on spectrometric characteristics of a high-pressure xenon gamma spectrometer, in: Proc. SPIE, vol. 3114, SPIE, Bellingham WA, 1997, pp. 499–504.
- [21] G. Tepper, Jon Losee, High resolution room temperature ionization chamber xenon gamma radiation detector, Nucl. Instrum. Methods Phys. Res. A 356 (1995) 339–346.
- [22] G.J. Mahler, B. Yu, G.C. Smith, W.R. Kane, J.R. Lemley, A portable gamma-ray spectrometer using compressed xenon, IEEE Trans. Nucl. Sci. 45 (1998) 1024–1033.
- [23] S.E. Ulin, V.V. Dmitrenko, A.E. Bolotnikov, Priby i Tekhnika Eksperimenta 2 (1994) 25–31.
- [24] V.V. Dmitrenko, I.V. Chernysheva, V.M. Gratchev, O.N. Kondakova, K.V. Krivova, S.E. Ulin, Z.M. Uteshev, K.F. Vlasik, Vibrostability of high pressure xenon gamma-ray detectors, IEEE Trans. Nucl. Sci. 47 (2000) 939–943.
- [25] V.V. Dmitrenko, A.G. Dvorniyak, V.M. Gratchev, O.N. Kondakova, K.V. Krivova, A. Yu Papchenko, D.V. Sokolov, S.E. Ulin, Z.M. Uteshev, K.F. Vlasik, A thermostable high pressure xenon gamma-ray detector for monitoring concentration of KCl during fertilizer manufacturing, Nucl. Instrum. Methods Phys. Res. A 422 (1999) 326–330.
- [26] S. Ottini-Hustache, C. Monsanglant-Louvet, S. Haan, V. Dmitrenko, S. Ulin, HPXe ionization chambers for γ spectrometry at room temperature, Nucl. Instrum. Methods Phys. Res. B 213 (2004) 279–283.
- [27] F. Lebrun, J.-P. Leray, P. Laurent, P. De Antoni, C. Blondel, A CdTe gamma-camera for the space observatory INTEGRAL: software charge-loss corrections, Nucl. Instrum. Methods Phys. Res. A 380 (1996) 414–418.
- [28] F. Resnati, U. Gendotti, R. Chandra, A. Curioni, G. Davatz, H. Friederich, A. Gendotti, L. Goeltl, R. Jebali, D. Murer, A. Rubbia, Suitability of high-pressure xenon as scintillator for gamma ray spectroscopy, Nucl. Instrum. Methods Phys. Res. A 715 (2013) 87–91.
- [29] A. Minamino, K. Abe, Y. Ashie, J. Hosaka, K. Ishihara, K. Kobayashi, Y. Kosho, C. Mitsuda, S. Moriyama, M. Nakahata, Y. Nakajima, T. Namba, H. Ogawa, H. Sekiya, M. Shiozawa, Y. Suzuki, A. Takeda, Y. Takeuchi, K. Taki, K. Ueshima, Y. Ebizuka, A. Ota, S. Suzuki, H. Hagiwara, Y. Hashimoto, S. Kamada, M. Kikuchi, N. Kobayashi, T. Nagase, S. Nakamura, K. Tomita, Y. Uchida, Y. Fukuda, T. Sato, K. Nishijima, T. Maruyama, D. Motoki, Y. Itow, Y.D. Kim, J.I. Lee, S.H. Moon, K.E. Lim, J.P. Cravens, M.B. Smy, Self-shielding effect of a single phase liquid xenon detector for direct dark matter search, Astroparticle Phys. 35 (2012) 609–614.
- [30] K. Ueshima, K. Abe, K. Hiraide, S. Hirano, Y. Kishimoto, K. Kobayashi, Y. Kosho, J. Liu, K. Martens, S. Moriyama, M. Nakahata, H. Nishiie, H. Ogawa, H. Sekiya, A. Shinozaki, Y. Suzuki, A. Takeda, M. Yamashita, K. Fujii, I. Murayama, S. Nakamura, K. Otsuka, Y. Takeuchi, Y. Fukuda, K. Nishijima, D. Motoki, Y. Itow, K. Masuda, Y. Nishitani, H. Uchida, S. Tasaka, H. Ohsumi, Y.D. Kim, Y.H. Kim, K.B. Lee, M.K. Lee, J.S. Lee, Scintillation-only based pulse shape discrimination for nuclear and electron recoils in liquid xenon, Nucl. Instrum. Methods Phys. Res. A 659 (2011) 161–168.
- [31] K. Abe, K. Hieda, K. Hiraide, S. Hirano, Y. Kishimoto, K. Kobayashi, S. Moriyama, K. Nakagawa, M. Nakahata, H. Ogawa, N. Oka, H. Sekiya, A. Shinozaki, Y. Suzuki, A. Takeda, O. Takachio, K. Ueshima, D. Umemoto, M. Yamashita, B.S. Yang, S. Tasaka, J. Liu, K. Martens, K. Hosokawa, K. Miuchi, A. Murata, Y. Onishi, Y. Otsuka, Y. Takeuchi, Y.H. Kim, K.B. Lee, M.K. Lee, J.S. Lee, Y. Fukuda, Y. Itow, K. Masuda, Y. Nishitani, H. Takiya, H. Uchida, N.Y. Kim, Y.D. Kim, F. Kusaba, D. Motoki, K. Nishijima, K. Fujii, I. Murayama, S. Nakamura, Light WIMP search in XMASS, Phys. Lett. B 719 (2013) 78–82.
- [32] E. Aprile, A. Curioni, K.L. Giboni, M. Kobayashi, S. Zhang, Compton imaging of MeV gamma-rays with the liquid xenon gamma-ray imaging telescope (LXEGRIT), Nucl. Instrum. Methods Phys. Res. A 593 (2008) 414–425.
- [33] S. Kobayashi, N. Hasebe, T. Hosojima, T. Igarashi, M.-N. Kobayashi, M. Mimura, T. Miyachi, M. Miyajima, K.N. Pushkin, H. Sakaba, C. Tezuka, T. Doke,

- E. Shibamura, A new generation γ -ray camera for planetary science applications: high pressure xenon time projection chamber, *Adv. Space Res.* 37 (2006) 28–33.
- [34] A. Bolozdynya, V. Egorov, A. Koutchenkov, G. Safronov, G. Smirnov, S. Medved, V. Morgunov, A high pressure xenon self-triggered scintillation drift chamber with 3D sensitivity in the range of 20–140 keV deposited energy, *Nucl. Instrum. Methods Phys. Res. A* 385 (1997) 225–238.
- [35] J.L. Lacy, A. Athanasiades, N.N. Shehad, L. Sun, T.D. Lyons, C.S. Martin, L. Bu, Cylindrical high pressure xenon spectrometer using scintillation light pulse correction, in: Proc., IEEE Nuclear Science Symposium, vol. 1, IEEE, New York, 2004, pp. 16–20.
- [36] P.N. Luke, Unipolar charge sensing with coplanar electrodes-application to semiconductor detectors, *IEEE Trans. Nucl. Sci.* 42 (1995) 207–213.
- [37] S.D. Kiff, Z. He, G.C. Tepper, Improving spectroscopic performance of a coplanar-anode high-pressure xenon gamma-ray spectrometer, *IEEE Trans. Nucl. Sci.* 54 (2007) 1263–1270.
- [38] A.E. Bolotnikov, R. Austin, A. Bolozdynya, J.D. Richards, Virtual Frisch-grid ionization chambers filled with high-pressure Xe, in: Proc., SPIE, vol. 5540, SPIE, Bellingham WA, 2004, pp. 216–224.
- [39] R.A. Austin, High-pressure xenon detector development at Constellation Technology Corporation, *Nucl. Instrum. Methods Phys. Res. A* 579 (2007) 58–61.
- [40] G. Tepper, J. Losee, R. Plamer, A cylindrical xenon ionization chamber detector for high resolution, room temperature gamma radiation spectroscopy, *Nucl. Instrum. Methods Phys. Res. A* 413 (1998) 467–470.
- [41] R. Kessick, G. Tepper, A hemispherical high-pressure xenon gamma radiation spectrometer, *Nucl. Instrum. Methods Phys. Res. A* 490 (2002) 243–250.
- [42] S.D. Kiff, Z. He, G.C. Tepper, A new coplanar-grid high-pressure xenon gamma-ray spectrometer, *IEEE Trans. Nucl. Sci.* 52 (2005) 2932–2939.
- [43] A.E. Bolotnikov, G. Smith, G.J. Mahler, P.E. Vanier US Patent, US7858949 B2, 2008.
- [44] É. Barat, T. Dautremer, T. Montagu, J.-C. Trama, A bimodal Kalman smoother for nuclear spectrometry, *Nucl. Instrum. Methods Phys. Res. A* 567 (2006) 350–352.
- [45] LANL Rep. No. LA-CP-11-00438, in: D.B. Pelowitz (Ed.), MCNPX User's Manual, Version 2.7.0, Los Alamos National Laboratory, 2011.
- [46] I. Giomataris, I. Irastorza, I. Savvidis, S. Andriamonje, S. Aune, M. Chapellier, Ph Charvin, P. Colas, J. Derre, E. Ferrer, A novel large-volume spherical detector with proportional amplification read-out, *J. Inst.* 3 (2008), P09007.